Northumbria Research Link

Improvement to thin film CdTe solar cells with controlled back surface oxidation

S. L. Rugen-Hankey[1], A. J. Clayton[1*], V. Barrioz[1], G. Kartopu[1], S. J. C. Irvine[1], J. D. McGettrick[2], D. Hammond[2]

[1]Centre for Solar Energy Research, Glyndwr University St Asaph, OpTIC, Denbighshire, LL17 0JD, UK
[2]Research & Development, Tata Steel, Rotherham, UK
*Corresponding author email: a.clayton@glyndwr.ac.uk

Abstract

Thin film CdTe solar cells were produced by MOCVD, at atmospheric pressure, under a hydrogen atmosphere (i.e. oxygen-free). Window layer alloying with zinc (forming $Cd_{1-x}Zn_xS$) and extrinsic p-type doping with arsenic (giving CdTe:As) have been used to improve photovoltaic solar cell performances, but as-grown MOCVD-CdTe PV cells are still typically characterised by low V_{oc} (~620 to 690 mV). Post-deposition annealing in air for 30 minutes at low temperature (170 °C) prior to evaporation of the back contacts led to significant increases in V_{oc} and FF. XPS measurements revealed back surface oxidation, resulting in formation of Te-O species. This was also the case for a device aged under ambient laboratory conditions. Extended annealing in air of a fresh device, for up to 180 minutes, continued to improve both V_{oc} and FF. At longer anneal times the V_{oc} remained relatively stable whilst the FF started to deteriorate. External quantum efficiency showed loss of photocurrent generation after excessive oxidation prior to back contact metallisation. Controlled back surface oxidation resulted in V_{oc} values exceeding 800 mV and a best cell efficiency of 15.3%.

Key words: CdTe; thin film; photovoltaics; open-circuit voltage; MOCVD

1. Introduction

Thin film cadmium telluride (CdTe) photovoltaic (PV) solar cells have been an established technology for the last 40 years [1] and have been successfully used in commercial solar module production [2]. CdTe has the largest share of the thin film PV market [3] which can be attributed, in part, to its high absorption coefficient and near optimal band gap, as well as its relatively simple large scale manufacturing capability. The industrial interest in CdTe has resulted in a number of recent improvements to world record conversion efficiencies, currently at 20.4% for a 0.5 cm^2 cell, 19.6% for a 1 cm^2 cell and 17.5% for a module [4]. For thin film CdTe PV, there is more scope to enhance the open circuit voltage (V_{oc}) and fill factor (FF), with less opportunity to improve the short circuit current density (J_{sc}) due to the main losses having been accounted for [5] and the best current value of 29.5 mA cm^{-2} (0.5 cm^2 cell) [4] approaching the theoretical limit of 30.5 mA cm^{-2} [6].

Improvements to V_{oc} may be realised by increasing the CdTe acceptor concentration, which remains a challenge due to defect formation and the self-compensating nature of CdTe [7-11]. Carrier concentrations for polycrystalline CdTe are currently limited to ~10^{15} cm^{-3} and intentional doping will be necessary for higher levels to be realised. Group V elements

have been demonstrated [8,12-16] as effective acceptor dopants. For example, arsenic (As) has been used [12-16] as a shallow acceptor in CdTe via metal organic chemical vapour deposition (MOCVD) by introducing the dopant *in situ* during CdTe layer growth, offering controlled levels of dopant incorporation throughout the depth of the layer.

Increased As dopant concentration towards the back contact improves the ohmic characteristic of the metal contact [12]. Conventionally, copper (Cu) is added to the back contact metal, complemented typically with gold (Au) due to its high work function, followed by a thermal anneal in air. This enables the Cu to diffuse into the CdTe surface where it acts as a shallow acceptor producing a p^+-layer that interfaces with the back contact metal and increases V_{oc} [17-18]. Formation of Cu oxides also typically occurs during the back surface after annealing in air [19]. The highest V_{oc} values achieved to date with superstrate CdS/CdTe devices are of the order of 850-870 mV [2, 4]. For comparison, the best MOCVD $Cd_{1-x}Zn_xS$/CdTe devices have featured a moderate V_{oc} of only 690 mV [14].

The FF, on the other hand, is largely determined by the PV solar cell series (R_s) and shunt (R_{sh}) resistances. To maximise FF, the R_s must be kept as low as possible by reducing contact resistance and R_{sh} must be kept as high as possible by improving layer uniformity over the device and reducing the density of pin-holes. However, the V_{oc} can influence a change in FF if R_s and R_{sh} remain unchanged [20]. Current high-efficiency CdTe solar cells have been reported [2, 4] with FF values approaching ~80%.

This paper presents a study into the effects of post-growth annealing in air of thin film CdTe solar cell devices produced in a hydrogen (H_2) atmosphere by MOCVD prior to deposition of the metallic back contact. Increases to both V_{oc} and FF were observed after post-growth annealing in direct comparison to as-grown PV solar cells produced in the same device deposition, resulting in significant overall improvements to conversion efficiency. The enhanced PV solar cell performance is discussed with consideration to the changes that have taken place at the CdTe/back contact interface.

2. Experimental

Thin film $Cd_{1-x}Zn_xS$/CdTe solar cells were deposited onto commercial indium tin oxide (ITO) coated aluminosilicate glass substrates using atmospheric pressure (AP) MOCVD with a horizontally configured growth chamber and H_2 (99.995% minimum purity) carrier gas. The substrates were 5.0×7.5 cm^2 in area with ITO sheet resistance of 4 - 8 $\Omega/\square$ and were static within the deposition chamber. The $Cd_{1-x}Zn_xS$ window layer was 0.24 μm in thickness with as-grown (no $CdCl_2$ activation) Zn concentration (x) of 0.7 [16]. Extrinsic As doping was used to obtain CdTe with p-type conductivity, with concentration of ~2×10^{18} atoms/cm^3 for the bulk CdTe and ~1×10^{19} atoms/cm^3 for a highly doped CdTe layer interfacing with the back contact to effectively give a p^+-layer [14]. The total CdTe thickness was 2.25 μm. $CdCl_2$ activation was deposited *in situ* [21] after CdTe deposition and annealed under H_2 at 420 °C for 10 min to activate the device. Full experimental details can be found elsewhere [14, 16].

A series of device samples were cleaved from a 5.0×7.5 cm^2 area and subjected to different back surface treatments. This included an air anneal at 170°C in an oven for one sample, typically for 30 minutes and separately ageing another sample which was left under

laboratory ambient conditions for a number of months. Extended air anneals beyond 30 minutes were also carried out for another set of devices. Afterwards, Au back contact metallisation was performed by thermal evaporation at 3 - 4 × 10^{-5} mbar base pressure to complete the solar cell structure. This ensured that the Au back contact did not influence the study of the back surface treatment. The air annealed and/or aged samples were compared to as-grown counterparts which received no back surface annealing treatment, i.e. back contact metallisation occurred immediately after the device was produced. Solar cells 0.25 cm^2 in area were defined by evaporating Au through a shadow mask on to the differently treated p^+-CdTe surfaces. Current density – voltage (J-V) measurements of the solar cells were carried out within a day following the back contact deposition.

AM1.5 J-V curves were collected using an Abet Technologies Ltd. solar simulator with the light power density calibrated using a Fraunhofer ISE certified c-Si reference cell. External quantum efficiency (EQE) measurements were carried out using a Bentham spectral response system under unbiased conditions over the spectral range 0.3 - 1 µm. The system response was corrected by scanning the output of a c-Si reference detector. X-ray photoelectron spectroscopy (XPS) was carried out using a Thermo VG Scientific instrument with an Alpha 110 hemispherical analyser and aluminium anode. A spot size of 5 mm was used for large area characterisation. Voltage was set to 12 kV with beam current of 6.67 mA giving a power of 80 W. The inelastic mean free path of electrons in a solid limits the practical sampling depth of XPS to <<10nm [22], ensuring that signals are from the surface region and ignore the bulk material composition. Survey scans were collected between 0 and 1100 eV at intervals of 0.5 eV and pass energy of 50 eV with 10 repeat scans averaged out using a dwell time per point of 20 ms.

3. Results and Discussion

The following sections compare J-V parameters between equivalent as-grown devices followed by different post-growth treatments and presented in terms of the chemical modifications occurring at the CdTe/Au interface as determined by XPS surface measurements. It is to be noted that the $Cd_{1-x}Zn_xS$/CdTe PV devices annealed in air at 170°C had back contact metallisation carried out after cooling to laboratory temperature. The aged device was left in a sample box under ambient laboratory conditions for 2½ months before the back contacts were evaporated on to the CdTe surface.

3.1 Current density - voltage (J-V) parameters

The mean J-V results with best cell conversion efficiencies for the devices that underwent the different post-growth treatments are shown in Table 1.

Device	J_{sc} (mA/cm^2)	V_{oc} (mV)	FF (%)	η (%)	Best η (%)
as-grown	25.0 ± 0.5	680 ± 10.4	69.4 ± 1.6	11.8 ± 0.2	12.1
30 min. anneal	25.4 ± 0.6	768 ± 0.5	75.5 ± 1.7	14.7 ± 0.6	15.3
60 min. anneal	24.3 ± 0.3	808 ± 0.0	73.2 ± 0.5	14.4 ± 0.1	14.6
aged	25.2 ± 0.4	788 ± 0.0	70.7 ± 7.0	14.0 ± 1.4	14.7

Table 1: Mean J-V results showing standard deviation and best cell efficiencies for 0.25 cm^2 Cd$_{1-x}$Zn$_x$S/CdTe solar cells, with different back surface treatments; as-grown (8 cells); air annealed for 30 min. (4 cells); air annealed for 60 min. (4 cells); aged in ambient laboratory conditions (8 cells).

The air annealed and the aged devices have significantly enhanced V_{oc} in comparison to the as-grown device as shown in Table 1. For the device air annealed for 60 min. the V_{oc} has increased by more than 100 mV. A large increase in V_{oc} was also observed for the aged device. The increase in conversion efficiency from the aged device can solely be attributed to the increase in V_{oc}, while the combined increase in V_{oc} and FF for the air annealed devices resulted in higher PV conversion efficiencies. A number of subsequent devices were produced and either subjected to the air anneal treatment or left as-grown, prior to back contact metallisation, to evaluate whether the improved PV performance after air annealing was reproducible. Each time, V_{oc} and FF were boosted following the air anneal treatment.

Figure 1 shows J-V curves of the cells with highest conversion efficiency (η) taken from each of the 4 devices represented in Table 1, where the improvement in V_{oc} for the air annealed and aged devices can be clearly observed. As shown in Figure 1, the J-V curve for the 30 min. air annealed PV solar cell displays superior diode characteristics, reflected by its higher FF. Also, clearly visible is the higher V_{oc} (808 mV) after air annealing for 60 min.
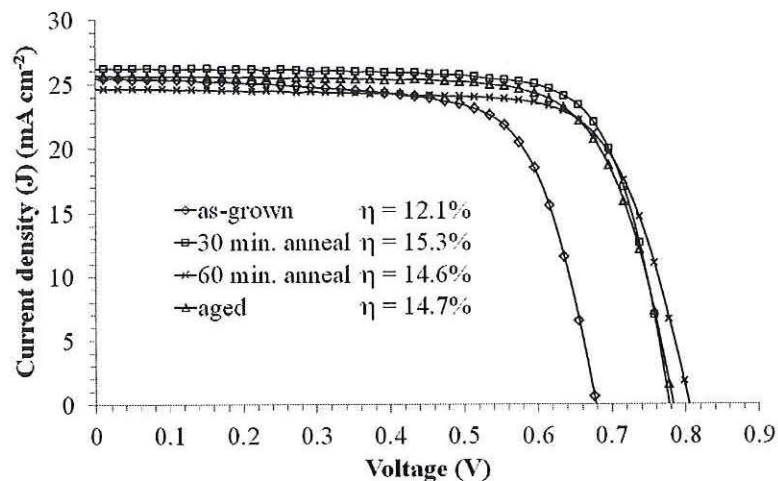

Figure 1: J–V curves for best Cd$_{1-x}$Zn$_x$S/CdTe solar cells from devices subjected to different post-growth treatments; as-grown; air annealed for 30 min.; air annealed for 60 min.; aged in laboratory ambient.

Another set of device samples were produced to include an anneal in an inert atmosphere. Annealing in nitrogen for 30 min. at 170°C was carried out as the post-deposition treatment for one device, with comparison to an as-grown device and a device air annealed at 170°C for 30 minutes. The nitrogen had a purity of 99.999 % with oxygen impurity $< 5 \times 10^{-4}$ % and moisture level $< 2 \times 10^{-4}$ %. Enhancement of V_{oc} and FF was again observed for the air annealed device, but no improvement was observed after an equivalent anneal in nitrogen. The process was further investigated using XPS to look at chemical changes at the back surface and in particular formation of oxides under air annealing.

3.2 XPS characterisation of the CdTe back surface

XPS characterisation was used to determine the chemical changes occurring at the CdTe back surface, by measuring a new set of device samples, leaving one as-grown and the other subjected to post-growth annealing in air. XPS was also carried out on the aged sample, at which stage it had been left under ambient laboratory conditions for 5 months. A section of each device without Au was used to characterise the chemical composition of the CdTe surface in each case. The measurements were made a few days after the as-grown and air annealed devices were produced in order to limit additional changes to the back surface, observed after ageing.

Figure 2 represents the core level peaks determined from the XPS measurements showing binding energies for Te $3d_{3/2}$ (573-577eV), Te $3d_{5/2}$ (584-587eV), O 1s (533 eV), Cd $3d_{3/2}$ (415 eV) and Cd $3d_{5/2}$ (409 eV), including that for C 1s (285 eV) which is consistent with what has been reported previously [23].
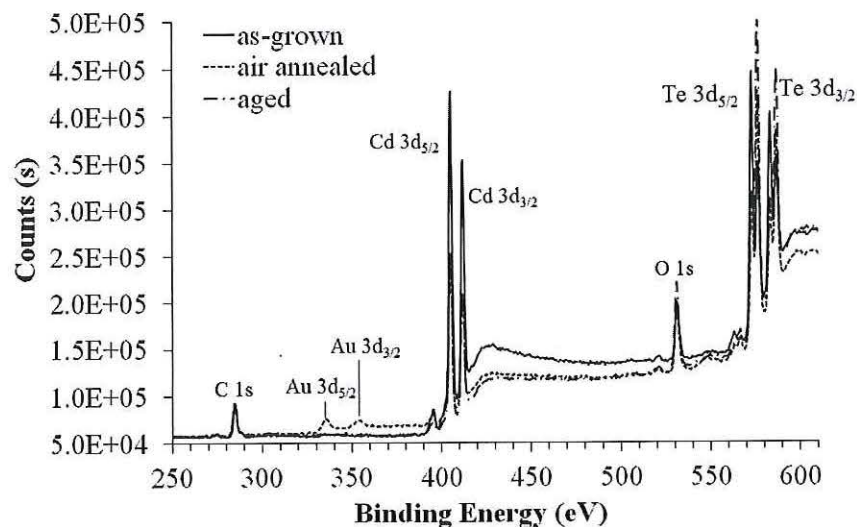

Figure 2: Core level binding energy peaks from XPS measurements at the back surface of $Cd_{1-x}Zn_xS/CdTe$ devices following different post-growth treatments: as-grown, air annealed (170°C, 30 min) and aged under ambient laboratory conditions for 5 months.

The region corresponding to the Te $3d_{5/2}$ and Te $3d_{3/2}$ binding energies has been expanded in Figure 3, and shows that each peak is split into two. The peaks at 573 eV (Te $3d_{5/2}$) and 583.5 eV (Te $3d_{3/2}$) are from Te associated with Cd whilst the higher binding energy peaks at 576.5 eV (Te $3d_{5/2}$) and 587 eV (Te $3d_{3/2}$) are due to Te associated with O. [23]. The Te(Cd) peak dominates for the as-grown device but diminishes for the air annealed and aged devices as the Te(O) peak increases. Nevertheless, the as-grown device still has Te(O) peaks present. This can only be due to the transition that occurred between the MOCVD process carried out under H_2 (oxygen-free) and the XPS measurements, as the device was not stored under vacuum. Therefore, even though this device was considered to be as-grown, the initial stage of ageing had occurred. For the intentionally (strongly) aged device the Te(O) peak is most prevalent whilst the Te(Cd) peak has reduced more significantly than for the air annealed device. The larger Te(O) peaks relative to the Te(Cd) peaks for the air annealed and intentionally aged devices confirm an oxidation process is occurring at the CdTe back surface prior to back contact metallisation.
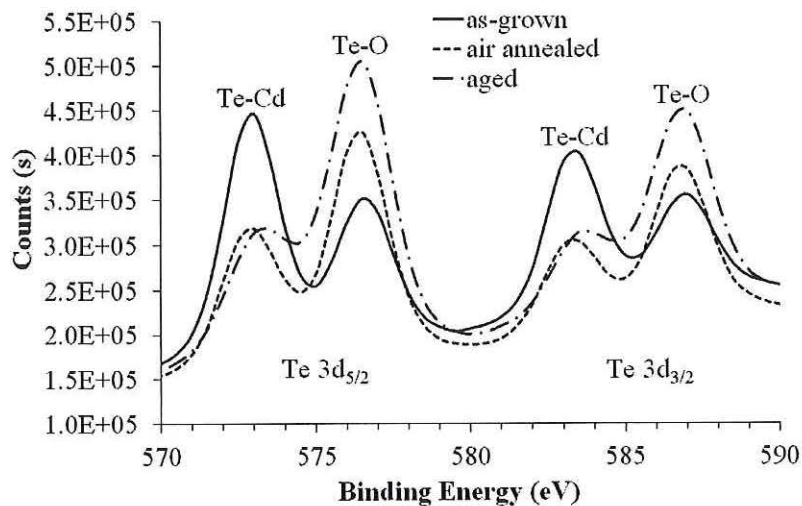

Figure 3: Expanded region of the XPS binding energies for the Te 3d peaks from measurements at the back surface of $Cd_{1-x}Zn_xS$/CdTe devices following different post-growth treatments: as-grown, air annealed (170°C, 30 min.) and aged under ambient laboratory conditions for 5 months.

The binding energy peaks for Cd $3d_{3/2}$ (415 eV) and Cd $3d_{5/2}$ (409 eV) have been expanded in Figure 4 showing no double peak formation as was the case for the Te 3d peaks displayed in Figure 3. Therefore, no information presents itself with the XPS measurements as to whether Cd-O bonds were also forming at the back CdTe surface of the devices. This is in agreement with what has been reported [23] previously relating to the formation of $CdTeO_3$ which does not result in a shift in binding energies.
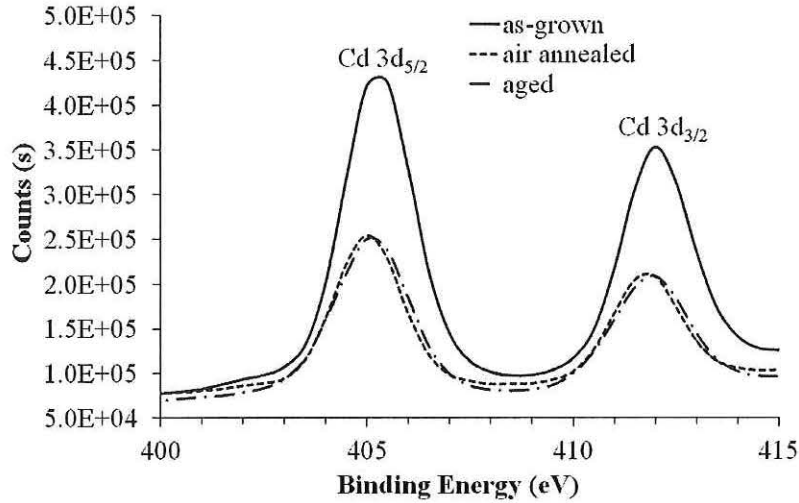
Figure 4: Expanded region of the XPS binding energies for the Cd 3d peaks from measurements at the back surface of $Cd_{1-x}Zn_xS/CdTe$ devices following different post-growth treatments; as-grown; air annealed (170°C, 30 min.); aged under ambient laboratory conditions for 5 months.

The XPS peaks were quantified to determine the elemental composition at the CdTe surface, as shown in Table 2. The Te concentration has remained relatively stable for each of the 3 devices receiving different back surface treatments. The as-grown device shows the presence of oxygen at the surface but there are increases in oxygen content for the air annealed and aged devices. Also of interest is the significant difference in Cd content at the surface between the as-grown device and air annealed and aged devices. Both the annealed and aged devices have half the Cd content as the as-grown device, effectively giving a Te-rich back surface. This will increase the p-type character at the back contact interface improving the ohmic properties. It cannot be deduced whether this is a consequence of back surface anneal treatments and more data would have to be collected for other device back surface compositions before any deductions were made.

Element peak	As-grown (at. %)	Annealed (at. %)	Aged (at. %)
O 1s	28.0	34.2	39.6
C 1s	30.8	34.5	29.1
Te 3d$_{5/2}$	21.0	21.4	21.4
Cd 3d$_{5/2}$	20.2	9.9	9.9

Table 2: XPS results showing quantified surface composition at the CdTe back surface for devices as-grown; air annealed for 30 min.; aged in ambient laboratory conditions.

The XPS results have revealed that air annealing effectively acts as an *accelerated* ageing process by the formation of a back surface oxide. The improvement of the V_{oc} and FF can be attributed to this back surface oxide through the following possible mechanisms:

1. Reducing shunt paths at grain boundaries.
2. Reducing the density of recombination centres at the back surface which will improve minority carrier lifetime [9].
3. Increase in back surface acceptor concentration to increase the back surface field.

These possible mechanisms could be investigated in a subsequent study using time-resolved photoluminescence, comparing as-grown CdTe devices with devices having received air annealing treatment.

Surface oxides were also reported [24] to form during the $CdCl_2$ annealing treatment of CdTe devices when carried out in the presence of O_2. The oxides were determined to be detrimental to PV solar cell performance, with short annealing times being preferred. Similarly, depositing CdTe in the presence of O_2 by close spaced sublimation (CSS) resulted [8] in improved V_{oc} when high O_2 partial pressures were used. It was inferred that the use of O_2 during the CSS-CdTe deposition process enhanced p-type doping. The oxidation process after air annealing could be considered to extend into the grain boundaries with additional contribution to the acceptor concentration, where the As (dopant) tends to segregate [25]. The influence of the air anneal on carrier concentration will be assessed by capacitance – voltage (C-V) measurements in a further study.

The MOCVD process employed here [12-16] used a H_2 atmosphere for deposition of all the layers as well as the *in situ* $CdCl_2$ anneal treatment, meanwhile Au back contact metallisation was carried out under high vacuum, i.e. oxygen-free environment. Unintentional oxidation inevitably occurs during transition between stages of device processing for as-grown MOCVD-CdTe devices but is eliminated between the formation of the window and absorber layers. The post-growth air annealing treatment has led to significant improvement to PV solar cell performance and has been determined by the authors to be a crucial step in processing MOCVD-CdTe devices. Further investigation into the optimisation of annealing in air is reported in the following section.

3.3 Evolution of J-V parameters with air annealing

A further thin film CdTe device (5.0×7.5 cm^2 in area) was produced, with a row of 4 as-grown PV solar cells before exposing them to different periods of air annealing (170°C) ranging from 30 to 420 minutes prior to evaporation of further rows of Au back contacts. J-V and EQE measurements on each row of 4 cells were carried out before the subsequent air anneals. The annealing stages were carried out immediately after the as-grown device had been produced and characterised until the CdTe device had been air annealed for a total of 420 minutes. The J-V results for all these cells are shown in Figure 5.
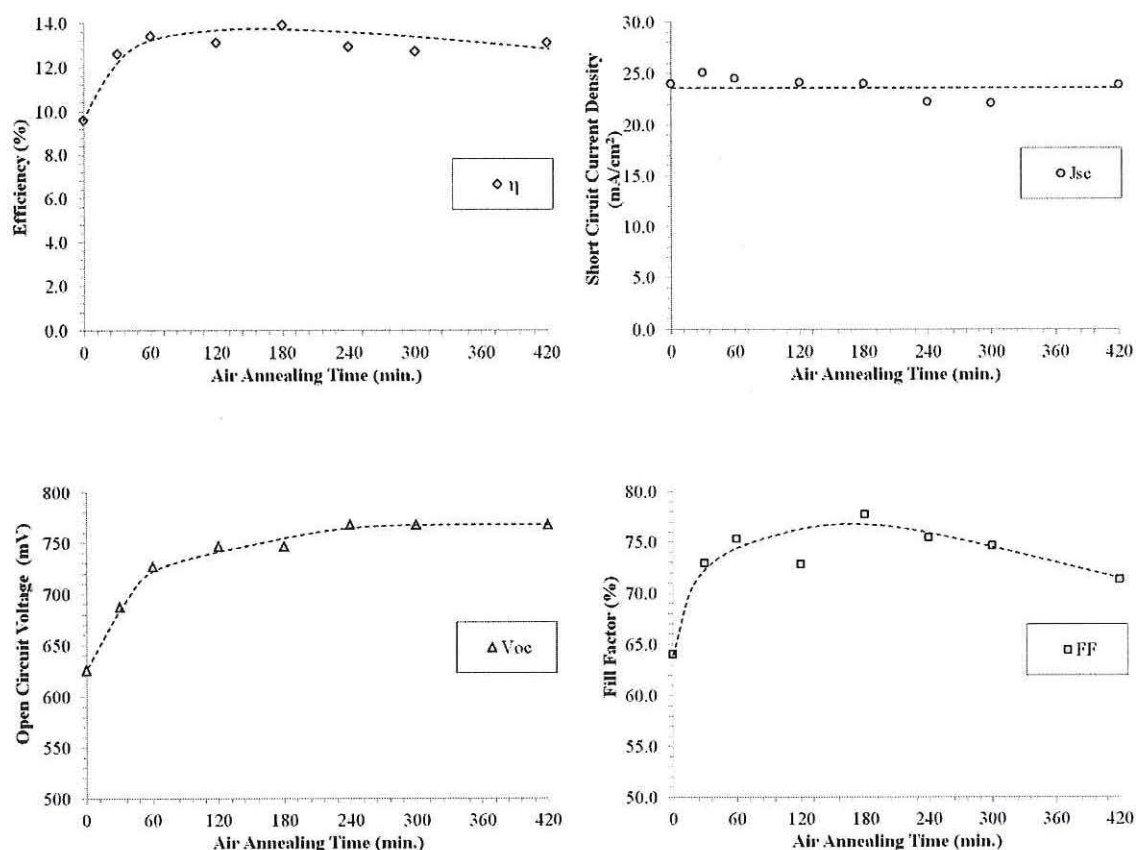
Figure 5: J-V results showing η (%), J_{sc} (mA/cm^2), V_{oc} (mV) and FF (%) for a thin film CdTe PV solar cell device 5.0 × 7.5 cm^2 in area, with rows of 4 Au 0.25 cm^2 contacts evaporated on to the CdTe back surface after the accumulated air annealing treatment times.

Extending the CdTe device annealing in air up to 240 min. led to incremental increases in V_{oc}, which then remained stable up to an anneal time of 420 min. Although there is uncertainty of the mechanism at this stage, the results show that a certain degree of oxide formation at the back surface is essential for boosting V_{oc} for these CdTe solar cell devices.

The FF has also increased after air annealing comparatively to cells processed on the as-grown device. The improvement in FF follows an irregular trend up to 180 minutes air annealing due to fluctuation in R_s and R_{sh} which might be more process dependant. FF started to drop beyond 180 minutes annealing in air, whilst V_{oc} continued to rise. The fall in FF corresponded to the changes in R_s and R_{sh} at the longer annealing times. From 240 min. of air annealing R_s began to rise. This could be expected to continue with further annealing and the formation of a thicker layer of insulating oxide. R_{sh} on the other hand had reduced after 60 minutes of air annealing and continued to reduce up to 180 minutes, after which it remained relatively stable.

Figure 6 shows EQE evolution for the same set of cells represented in Figure 5. Some loss of EQE occurs at longer wavelength consistent towards the trend for some deterioration for the longer anneals. In general photocurrent generation falls as the air annealing treatment is extended beyond 60 min., and then remained relatively stable up to the 180 minute anneal.

The spectral range of the EQE curves did not correlate with the high J_{sc} values shown in Table 1. A small spectral mismatch between the Si calibration cell and CdTe test cells resulted in an approximate 2 mA/cm^2 increase in the J_{sc} values reported in Table 1.
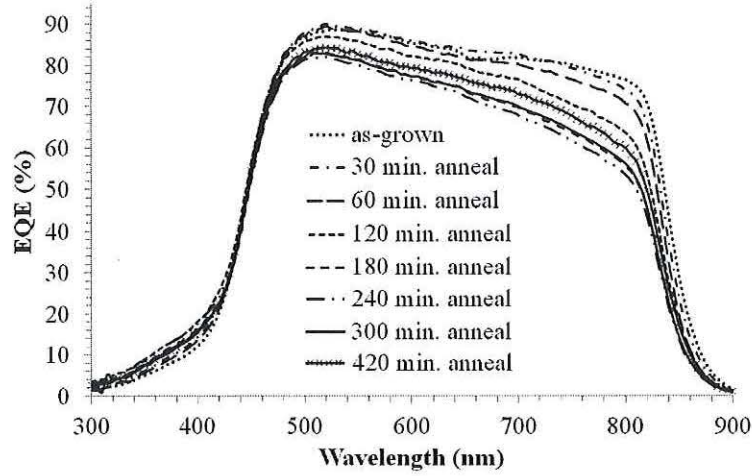

Figure 6: EQE curve evolution of CdTe PV solar cells on the same 5.0 × 7.5 cm^2 device after varying air annealing times prior to back contact metallisation.

The optimal back surface anneal treatment in order to produce the best J-V parameters requires preservation of the FF (keeping the R_s low whilst boosting the R_{sh}). Although V_{oc} continues to increase with a certain level of extended oxidation, FF begins to deteriorate.

4. Conclusions

Improvements to V_{oc} and FF have been demonstrated for MOCVD deposited CdTe PV solar cells produced under a H$_2$ atmosphere after low temperature air annealing, with direct comparison to equivalent PV solar cells on an as-grown CdTe device. The PV solar cell performance significantly increased after air annealing, prior to back contact metallisation. XPS revealed that Te-O species formed on the CdTe surface for all devices, with more intense peaks, implying more oxide, for the air annealed and aged device samples. The Te(Cd) peak dominated for the as-grown device, but Te(O) contribution increased for the air annealed and aged devices. Possible mechanisms for the improved PV solar cell performance include a reduction of shunt paths at the grain boundaries, decrease in recombination centres at the back surface improving minority carrier lifetime, or an increase in acceptor concentration at the back surface enhancing the back surface field. The effects of extended annealing times up to 420 minutes have been studied, with immediate air annealing, after the active layer deposition being preferred, for optimal PV solar cell performance. V_{oc} increased steadily before remaining stable with extended annealing. Improvements to FF were also observed, although at longer annealing times it started to deteriorate causing an overall drop

in efficiency. Nevertheless, it has been shown that there is a broad range of oxidation treatments that give significant enhancement in efficiency.

References

1 D. Bonnet and H. Rabenhorst, New results on the development of a thin film p-CdTe/n-CdS heterojunction solar cell, Proc. of 9th IEEE Photovoltaics Specialists Conference, Silver Spring, 1972, 129-131.

2 L. Kranz, S. Buecheler, A.N. Tiwari, Technological status of CdTe photovoltaics, Solar Energy Materials and Solar Cells 119 (2013) 278-280.

3 M. Marwede, A. Reller, Future recycling flows of tellurium from cadmium telluride photovoltaic waste, Resource Conservation and Recycling 69 (2012) 35–49.

4 M.A. Green, K. Emery, Y. Hishikawa, W. Warta, E.D. Dunlop, Solar cell efficiency tables (version 44), Progress in Photovoltaics: Research and Applications 22 (2014) 701-710.

5 J.R. Sites, Quantification of losses in thin-film polycrystalline solar cells, Solar Energy Materials and Solar Cells, 75 (2003) 243-251.

6 A. Bosio, N. Romeo, S. Mazzamuto, V. Canevari, Polycrystalline CdTe thin films for photovoltaic applications, Progress in Crystal Growth and Characterisation of Materials 52 (2006) 247-279.

7 R. W. Birkmire, B. E. McCandless, CdTe thin film technology: Leading thin film PV into the future, Current Opinion in Solid State and Materials Science 14 (2010) 139-142.

8 H. Zhao, Alvi Farah, D. Morel, C.S. Ferekides, The effect of impurities on the doping and V_{oc} of CdTe/CdS thin film solar cells, Thin Solid Films 517 (2009) 2365-2369.

9 J. Sites, J. Pan, Strategies to increase CdTe solar-cell voltage, Thin Solid Films 515 (2007) 6099-6102.

10 J. Versluys, P. Clauws, P. Nollet, S. Degrave, M. Burgelman, Characterisation of deep defects in CdS/CdTe thin film solar cells using deep level transient spectroscopy, Thin Solid Films 451-452 (2004) 434-438.

11 U.V. Desnica, Doping limits in II-VI compounds – Challenges, Progress in Crystal Growth and Characterisation of Materials 36 (1998) 291-357.

12 V. Barrioz, Y.Y. Proskuryakov, E.W. Jones, J.D. Major, S.J.C. Irvine, K. Durose, D.A. Lamb, Highly arsenic doped CdTe layers for the back contacts of CdTe solar cells, Materials Research Society Symposium Proceedings 1012 (2007) Y12-08.

13 V. Barrioz, S.J.C. Irvine, E.W. Jones, R.L. Rowlands, D.A. Lamb, In situ deposition of cadmium chloride films using MOCVD for CdTe solar cells, Thin Solid Films 515 (2007) 5808-5813.

14 S.J.C. Irvine, V. Barrioz, D. Lamb, E.W. Jones, R.L. Rowlands-Jones, MOCVD of thin film polycrystalline solar cells – Next-generation production technology?, Journal of Crystal Growth 310 (2008) 5198–5203.

15 Y.Y.Proskuryakov,K.Durose, J.D.Major, M.K. Al Turkestani, V. Barrioz, S.J.C. Irvine, E.W. Jones, Doping levels, trap density of states and the performance of co-

doped CdTe(As,Cl) photovoltaic devices, Solar Energy Materials and Solar Cells 93 (2009) 1572-1581.

16 G. Kartopu, A.J. Clayton, W.S.M. Brooks, S.D. Hodgson, V. Barrioz, A. Maertens, D.A. Lamb, S.J.C. Irvine, Effect of window layer composition in $Cd_{1-x}Zn_xS/CdTe$ solar cells, Progress in Photovoltaics: Research and Applications 22 (2014) 18-23.

17 A.D. Compaan, A. Gupta, S. Lee, S. Wang, J. Drayton, High efficicency, magetron sputtered CdS/CdTe solar cells, Solar Energy 77 (2004) 815-822.

18 S.H. Demtsu, D.S. Albin, J.R. Sites, W.K. Metzger, A. Duda, Cu-related recombination in CdS/CdTe solar cells, Thin Solid Films 516 (2008) 2251-2254.

19 S. Pookpanratana, X. Liu, N.R. Paudel, L. Weinhardt, M. Bär, Y. Zhang, A. Ranasinghe, F. Khan, M. Blum, A.D. Compaan, C. Heske, Effects of postdeposition treatments on surfaces of CdTe/CdS solar cells, Applied Physics Letters 97 (2010) 172109.

20 M.A. Green, Solar cell fill factors: General graph and empirical expressions, Solid State Electronics 24 (1981) 788-789.

21 V. Barrioz, S.J.C. Irvine. E.W. Jones, R.L. Rowlands and D.A. Lamb, *In situ* deposition of cadmium chloride films using MOCVD for CdTe solar cells, Thin Solid Films 515 (2007) 5808–5813.

22 M. P. Seah, W. A. Dench, Quantitative electron spectroscopy of surfaces: A standard data base for electron inelastic mean free paths in solids, Surface and Interface Analysis 1 (1979) 2-11.

23 P. Bartolo-Pérez, M.H. Farías, R. Castro-Rodríguez, J.L. Peña, F. Caballero-Briones, W. Cauich, XPS analysis of oxidation states of Te in CdTe oxide films grown by rf sputtering with an $Ar-NH_3$ plasma, Superficies Vacio 12 (2001) 8-11.

24 C.S. Ferekides, U. Balasubramanian, R. Mamazza, V. Viswanathan, H. Zhao, D.L. Morel, CdTe thin film solar cells: device and technology issues, Solar Energy 77 (2004) 823-830.

25 W.S.M. Brooks, S.J.C. Irvine, D.M. Taylor, Scanning Kelvin probe measurements on As-doped CdTe solar cells, Semiconductor Science and Technology 28 (2013) 10524, 1-6.